

Downlink Performance of Distributed Antenna Systems in MIMO Composite Fading Channel

Weiye Xu¹, Qingyun Wang¹, Ying Wang², Binbin Wu²

¹ School of Communication Engineering, Nanjing Institute of Technology, Nanjing, China,

² Department of Electronic Engineering, Nanjing University of Aeronautics and Astronautics, Nanjing, China

*Corresponding author: Weiye Xu

Received April 24, 2014; revised June 10, 2014; accepted July 7, 2014; published October 31, 2014

Abstract

In this paper, the capacity and BER performance of downlink distributed antenna systems (DAS) with transmit antenna selection and multiple receive antennas are investigated in MIMO composite channel, where path loss, Rayleigh fading and lognormal shadowing are all considered. Based on the performance analysis, using the probability density function (PDF) of the effective SNR and numerical integrations, tightly-approximate closed-form expressions of ergodic capacity and average BER of DAS are derived, respectively. These expressions have more accuracy than the existing expressions, and can match the simulation well. Besides, the outage capacity of DAS is also analyzed, and a tightly-approximate closed-form expression of outage capacity probability is derived. Moreover, a practical iterative algorithm based on Newton's method for finding the outage capacity is proposed. To avoid iterative calculation, another approximate closed-form outage capacity is also derived by utilizing the Gaussian distribution approximation. With these theoretical expressions, the downlink capacity and BER performance of DAS can be effectively evaluated. Simulation results show that the theoretical analysis is valid, and consistent with the corresponding simulation.

Keywords: Distributed antenna systems, ergodic capacity, outage capacity, BER, outage probability, composite channel

1. Introduction

As a promising technique for future wireless communications, the distributed antenna system (DAS) has received much interests in recent years [1][2][3][4][5][6][7][8][9][10]. In DAS, the distributed antennas are separated geographically and connected to a central control module via dedicated wires, fiber optics, or an exclusive radio frequency link. Compared to the traditional co-located antenna system (CAS), DAS can effectively exploit both the advantages of micro- and macro-diversity, and significantly improve the system capacity and cell coverage, and reduce power consumption. Recent studies on application of DAS have drawn considerable attention in both academic research and standardization activities like LTE-Advanced [8][9], DAS cellular system [6], and distributed multi-input multi-output (MIMO) [8]. Moreover, as a promising application, DAS may solve the problems arising from frequency selective channel and limited transmit power [10]. Besides, the antenna selection (AS) transmission scheme with maximal-ratio combining (MRC) is an effective diversity scheme to increase the performance while significantly decreasing the hardware complexity and cost [11][12]. Therefore, effective combination of DAS and AS technique will improve the system performance greatly with efficient hardware complexity and cost.

Many academic works have been done to analyze the capacity performance of DAS, and proved that DAS can enhance the system capacity effectively [13][14][15]. The impact of MRC-based macrodiversity on the capacity of code division multiple access (CDMA) DAS uplink is studied in [13]. The downlink capacity of DAS over Rayleigh fading and Nakagami fading in multicell environment are analyzed in [14] and [15], respectively. The closed-form expressions of ergodic capacity are derived in the above two references, but the derived expression in [14] has minor error, while [15] needs iterative calculation. For this, an accurate closed-form expression of ergodic capacity of downlink DAS in Nakagami fading multicell environment is derived in [16]. However, the above literatures do not consider the effect of shadow fading on the performance. Based on this, the ergodic capacity performance of downlink DAS is investigated in [17] by using different cooperation strategies, but the influence of noise is neglected for analysis simplicity. In [18], [19] and [20], by using a log-normal distribution to substitute the gamma-log-normal distribution, approximate expressions of the ergodic capacity are derived for downlink DAS over shadowed fading channel, where Rayleigh fading and Nakagami fading are respectively considered, but the derived theoretical capacity are not accurate enough to reflect the actual values, and the analysis is limited in single receive antenna case. By utilizing the high signal to noise ratio (SNR) analysis, a simple ergodic capacity expression is derived in [21], and can be close to the actual cell average ergodic capacity in high SNR (even in moderate SNR). By assuming double-sided spatial correlation, an analytical lower bound of the ergodic capacity of DAS in composite Rayleigh/lognormal fading channel is provided in [22], but the capacity is accurate in the low and high SNR regimes only. Considering that system outage probability is an important performance measure of communication systems, the outage performance of DAS in fading channel is studied in [23][24][25][26][27][28][29]. For the DAS uplink, the approximate outage probability is analyzed and derived for DAS in composite Rayleigh/lognormal fading channels [23][24], in composite Nakagami/lognormal fading channels [25], and in composite generalized-gamma /lognormal fading channels [26][27], where the mobile terminal (MT) is equipped with one antenna only. In [28], an approximate outage probability is derived for downlink DAS with single receive antenna in composite Rayleigh and lognormal fading channels [28]. In [29], a closed-form approximation of the outage

probability for the DAS downlink and uplink is derived, and this expression will be tight and valid only when the rate or the number of nodes and antennas of the system become large. Besides, [30] and [31] investigate the BER performance of DAS in composite fading channel, and give the approximate BER expressions in single-cell and multi-cell environment, respectively. However, the obtained BER in [30] is not accurate since it adopts the gamma distribution to approximate log-normal distribution for easy derivation, and the BER is not easy to calculate because of employing the complicated function (Meijer function). Whereas the derived BER in [31] is suitable for BPSK modulation only, and does not consider the superiority of AS scheme. If the AS is adopted, the derivation of average BER will become difficult.

Although in all these studies, the channel capacity and outage probability are well analyzed, the obtained capacity expressions in composite fading channel are not accurate because of using inaccurate approximation. Moreover, only limited work has been carried out for the BER and outage performance analysis of DAS downlink. Especially, the outage capacity of DAS over composite fading channels is not studied in the existing literatures. Motivated by the reasons above, we will address the performance analysis of downlink DAS with transmit antenna selection and multiple receive antennas in composite channel which takes path loss, lognormal shadowing and Rayleigh fading into account, and focus on the derivation of the ergodic capacity, average BER and outage capacity of downlink DAS in MIMO composite fading channel. In terms of the channel state information and maximum SNR criterion, a selection transmission scheme is presented to maximize the output SNR, i.e., only the ‘best’ distributed antenna is selected for data transmission. Based on this scheme and the performance analysis, using some numerical integrations (Gauss-Hermite integration, Gauss-Laguerre integration, etc.), the probability density function (PDF) and cumulative distribution function (CDF) of the effective output SNR of DAS are respectively obtained. With the obtained CDF and PDF, tightly-approximate closed-form expressions of ergodic capacity and BER of DAS are derived, respectively. These expressions have more accuracy than the existing ones. To analyze the outage performance of the system well, we also derive a tightly-approximate closed-form expression of outage probability for DAS for a given outage capacity. Meanwhile, a practical iterative algorithm based on Newton method for calculating the system outage capacity is proposed for a given outage probability. As a result, accurate outage capacity is achieved. Moreover, by utilizing the Gaussian distribution approximation, an approximate closed-form expression of outage capacity of DAS is also derived. With these theoretical expressions, the capacity and BER performance of DAS downlink can be effectively assessed. Computer simulation shows that the presented theoretical analysis is valid, and has the values very close to the simulated results.

The notations we use throughout this paper are as follows. Bold upper case and lower case letters denote matrices and column vectors, respectively. $E\{\cdot\}$ denotes the expectation. The superscripts $(\cdot)^T$ and $(\cdot)^H$ are used to stand for the transpose and Hermitian transpose, respectively.

2. System Model

In this paper, we consider a DAS with multiple remote antennas (RAs) and multiple receive antennas in a single cell whose covering area is approximated by a circle of radius R as shown in Fig. 1, the RAs are distributed in the cell and connected with the central base station (BS, also named as RA_0) via coaxial cables, fiber optics or radio links, where N_r RAs are considered, and the i -th RA is denoted as RA_i . The MT is equipped with N_t antennas, and it is assumed to

be independent and uniformly distributed in the cell as in [14] [21]. To improve the system performance, the antenna selection diversity scheme is employed for RAs. If RA_i is selected to transmit the signals, the received signals at MT can be expressed as

$$\mathbf{r}_i = \sqrt{P_i} \mathbf{h}_i b + \mathbf{w} = \sqrt{P_i} [h_i^{(1)}, h_i^{(2)}, \dots, h_i^{(N_r)}]^T b + \mathbf{w} \quad (1)$$

where $\mathbf{r}_i = [r_i^{(1)}, r_i^{(2)}, \dots, r_i^{(N_r)}]^T$, $r_i^{(j)}$ is the received signal from the j -th antenna at MT, P_i is the transmit power. $h_i^{(j)}$ is the element of channel vector \mathbf{h}_i , and it denotes the composite channel fading coefficient between RA_i and the j -th antenna of MT. b is the transmitted signal from RA_i with unity energy. \mathbf{w} is the noise vector, whose elements are independent, identically distributed (*i.i.d*) complex Gaussian random variables with zero-mean and variance σ_w^2 . $h_i^{(j)}$ can be modeled as [18][19].

$$h_i^{(j)} = \kappa_i^{(j)} \sqrt{L_i S_i} \quad (2)$$

where $\kappa_i^{(j)}$ represents the small-scale fading between RA_i and the j -th receive antenna of MT. For Rayleigh fading channel, $\{\kappa_i^{(j)}\}$ are modeled as independent complex Gaussian random variables with zero-mean and unit-variance. L_i and S_i denote the pass loss and shadowing effect between RA_i and MT. The path loss term L_i is expressed as $L_i = (d_r / d_i)^{\beta_i}$, where β_i is the path loss exponent, d_r is the reference distance and d_i represents the distance from RA_i to MT. The shadowing effect term S_i is log-normally distributed, and the mean of $10 \lg S_i$ is assumed to be zero (in dB). As a result, the PDF of S_i can be expressed as [32]

$$f_{S_i}(s) = \frac{\gamma}{\sqrt{2\pi}\sigma_i s} \exp\left(-\frac{(10 \lg s)^2}{2\sigma_i^2}\right) \quad (3)$$

where s is the variable of shadowing effect term S_i , σ_i (in dB) is the standard deviation of $10 \lg S_i$ and $\gamma = 10/\ln 10$.

According to (1) and (2), when single RA_i is selected, the output SNR after MRC can be obtained as

$$\rho_i = \sum_{j=1}^{N_r} \rho_i^{(j)} = \alpha_i \sum_{j=1}^{N_r} |\kappa_i^{(j)}|^2 \quad (4)$$

where $\rho_i^{(j)}$ denotes the instantaneous SNR at the j -th receive antenna, and $\alpha_i = P_i L_i S_i / \sigma_w^2$. From (4), it is shown that α_i is also log-normally distributed. Thus, by a transformation of random variables, its PDF can be given by

$$f_{\alpha_i}(x) = \frac{\gamma}{\sqrt{2\pi}\sigma_i x} \exp\left(-\frac{(10 \lg x - \nu_i)^2}{2\sigma_i^2}\right) \quad (5)$$

where $\nu_i = 10 \lg(P_i L_i / \sigma_w^2)$ is the mean of $10 \lg \alpha_i$. Considering that $\sum_{j=1}^{N_r} |\kappa_i^{(j)}|^2$ is chi-squared distribution with $2N_r$ degrees of freedom, the PDF of ρ_i can be obtained as

$$f_{\rho_i}(\rho) = \int_0^\infty \frac{\rho^{N_r-1}}{\Gamma(N_r) x^{N_r}} \exp\left(-\frac{\rho}{x}\right) \frac{\gamma}{\sqrt{2\pi}\sigma_i x} \exp\left(-\frac{(10 \lg x - \nu_i)^2}{2\sigma_i^2}\right) dx \quad (6)$$

Due to the difficulty of integration, (6) is not easy to calculate and obtain the closed form. For this reason, [18] and [19] resort to the log-normal distribution, and use it to approximate the Gamma-log-normal distribution in (6) and derive the closed-form PDF of ρ_i . Unfortunately, using this approximate PDF to derive the capacity and BER will result in the inaccuracy of the obtained theoretical formulae in some cases. For this, we will recalculate Eq.(6) using the numerical integration and the transformation of variable.

Let $t = (10 \lg x - \nu_i) / \sqrt{2\sigma_i^2}$, then (6) can be rewritten as

$$f_{\rho_i}(\rho) = \frac{1}{\Gamma(N_r)\sqrt{\pi}} \int_{-\infty}^{+\infty} \exp\left(-10^{-\frac{\sqrt{2}\sigma_i t + \nu_i}{10}} \rho\right) \rho^{N_r-1} \left(10^{-\frac{\sqrt{2}\sigma_i t + \nu_i}{10}}\right)^{N_r} \exp(-t^2) dt$$

$$\cong \frac{1}{\Gamma(N_r)\sqrt{\pi}} \sum_{n=1}^{N_p} H_n \exp(-\rho c_{in}) (\rho c_{in})^{N_r-1} c_{in}$$
(7)

where the Gauss-Hermite integration [33] is utilized, and $c_{in} = 10^{-[\sqrt{2}\sigma_i t_n + \nu_i]/10}$. t_n and H_n are the base point and weight factor of the N_p -order Hermite polynomial, respectively. Eq.(7) is a tightly approximate PDF, and has more accuracy than the provided approximate PDFs in [18][19].

From (7), we can obtain the CDF of ρ_i as follows:

$$F_{\rho_i}(\rho) = \int_0^\rho f_{\rho_i}(y) dy \cong 1 - \frac{1}{\sqrt{\pi}\Gamma(N_r)} \sum_{n=1}^{N_p} H_n \Gamma(N_r, \rho c_{in})$$
(8)

where $\Gamma(\cdot, \cdot)$ is the incomplete Gamma function [34].

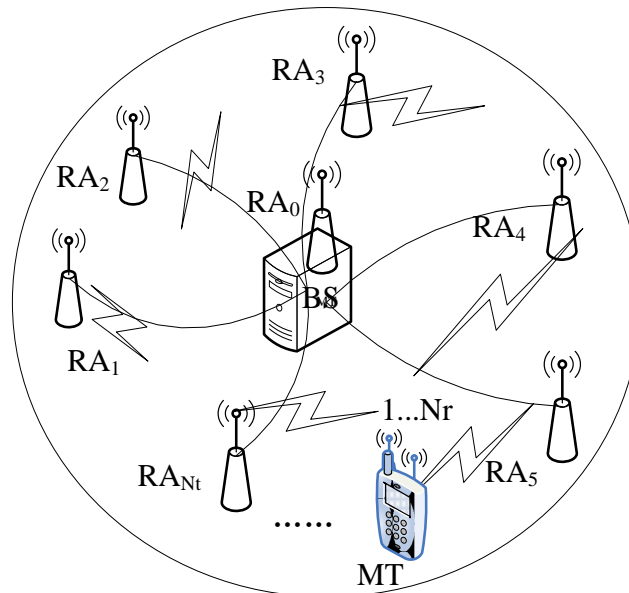


Fig. 1. Diagram of DAS structure.

3. Capacity performance analysis

3.1 Ergodic capacity

In this subsection, we will give the downlink capacity analysis of the DAS in a composite Rayleigh and lognormal shadowing fading channel. Ergodic capacity is an appropriate capacity metric for channels that vary quickly, or where the channel is ergodic over the time period of interest [35], it is equal to Shannon capacity in an Additive White Gaussian Noise (AWGN) channel with $\log_2(1+\rho)$, averaged over the distribution of ρ . Thus, the ergodic capacity can be expressed as

$$C_e = E\{C\} = E\{\log_2(1 + \rho)\} = \int_0^\infty f(\rho) \log_2(1 + \rho) d\rho \quad (9)$$

where $C = \log_2(1+\rho)$ is the channel capacity, and $f(\rho)$ is PDF of output SNR ρ .

According to the analyzed in section 2, the selective diversity scheme is applied to the transmitter, i.e., only one ‘best’ RA is selected for transmission to maximize the output SNR. Thus, we have: $\rho = \max\{\rho_0, \rho_1, \dots, \rho_{N_r}\}$. Considering large space among remote antennas, it is reasonable to assume that $\{\rho_i\}$ are independent. Hence, with (8), the CDF of ρ , $F(\rho)$, can be given by

$$F(\rho) = \prod_{i=0}^{N_r} F_{\rho_i}(\rho) \cong \prod_{i=0}^{N_r} \left[1 - \frac{1}{\sqrt{\pi}\Gamma(N_r)} \sum_{n=1}^{N_p} H_n \Gamma(N_r, \rho c_{in})\right] \quad (10)$$

Using (10) and (7) as well as (8), we can obtain the PDF, $f(\rho)$, as follows:

$$\begin{aligned} f(\rho) &= dF(\rho) / d\rho = \sum_{i=0}^{N_r} [f_{\rho_i}(\rho) \prod_{k=0, k \neq i}^{N_r} F_{\rho_k}(\rho)] \\ &\cong \sum_{i=0}^{N_r} \frac{1}{\Gamma(N_r)\sqrt{\pi}} \sum_{n=1}^{N_p} H_n e^{-\rho c_{in}} (\rho c_{in})^{N_r-1} c_{in} \prod_{k=0, k \neq i}^{N_r} \left[1 - \frac{1}{\sqrt{\pi}\Gamma(N_r)} \sum_{m=1}^{N_p} H_m \Gamma(N_r, \rho c_{im})\right] \end{aligned} \quad (11)$$

Substituting (11) into (9) yields

$$C_e \cong \sum_{i=0}^{N_r} \sum_{n=1}^{N_p} H_n \left[\int_0^{+\infty} \log_2(1 + \rho) \frac{c_{in}}{\Gamma(N_r)\sqrt{\pi}} (\rho c_{in})^{N_r-1} e^{-\rho c_{in}} \prod_{k=0, k \neq i}^{N_r} F_{\rho_k}(\rho) d\rho \right] \quad (12)$$

Utilizing the transformation of variable $z = \rho c_{in}$, and Gaussian-Laguerre integration in [33], (12) can be changed to

$$\begin{aligned} C_e &\cong \sum_{i=0}^{N_r} \sum_{n=1}^{N_p} H_n \int_0^{+\infty} \log_2\left(1 + \frac{z}{c_{in}}\right) \frac{z^{N_r-1}}{\Gamma(N_r)\sqrt{\pi}} \left[\prod_{k=0, k \neq i}^{N_r} F_{\rho_k}\left(\frac{z}{c_{in}}\right) \right] e^{-z} dz \\ &= \sum_{i=0}^{N_r} \sum_{n=1}^{N_p} H_n \sum_{u=1}^{N_q} A_u \log_2\left(1 + \frac{z_u}{c_{in}}\right) \frac{z_u^{N_r-1}}{\Gamma(N_r)\sqrt{\pi}} \prod_{k=0, k \neq i}^{N_r} F_{\rho_k}\left(\frac{z_u}{c_{in}}\right) \end{aligned} \quad (13)$$

where $F_{\rho_k}(\rho)$ is the CDF of ρ_k , as shown in (8), $\{A_u\}$ are the weights associated with the zeros $\{z_u\}$ of the one dimensional N_q -th order Laguerre polynomial [33]. Eq.(13) is a tightly

approximate closed-form expression of ergodic capacity of downlink DAS in composite fading channel, it has more accuracy than the existing expressions in [18][19] because the latter employs the approximate PDF for capacity derivation. It is shown that the derived (13) is in good agreement with the simulation.

3.2 Outage capacity

The outage capacity and probability are important performance measure of communication systems in fading channels, and are also important to network scheduling and antenna layout [23][24][25][26][27]. However, the related research is relatively less, especially the outage capacity analysis is much less. For this reason, we will give the outage performance analysis of the DAS downlink in a composite channel, and derive the closed-form outage capacity and probability. Since the channel capacity is a random variable, it is meaningful to consider its statistical distribution. A useful measure of statistical characteristic is the outage capacity [36]. For the given outage capacity C_o , $P(C_o)$ is defined as the outage probability that the channel capacity $C = \log_2(1+\rho)$ falls below C_o . Thus, the outage probability can be expressed as

$$\begin{aligned} P(C_o) &= \text{Pr ob}(C \leq C_o) = \text{Pr ob}(\rho \leq 2^{C_o} - 1) \\ &= \int_0^{2^{C_o} - 1} f(\rho) d\rho = F(2^{C_o} - 1) \end{aligned} \quad (14)$$

Substituting (10) into (14) gives

$$P(C_o) = F(2^{C_o} - 1) \cong \prod_{i=0}^{N_t} \left[1 - \frac{1}{\sqrt{\pi} \Gamma(N_r)} \sum_{n=1}^{N_p} H_n \Gamma(N_r, (2^{C_o} - 1) c_{in}) \right] \quad (15)$$

Eq.(15) is a tightly-approximate closed-form expression of outage probability of downlink DAS in composite fading channel for the given outage capacity C_o , which is shown to accord with the simulation.

For a given outage probability $\varepsilon = P(C_o)$, we propose a practical iterative algorithm based on Newton's method for finding the outage capacity C_o . In the following, we express solving the outage capacity from (15) as finding the root of $G(C_o) = 0$ with

$$\begin{aligned} G(C_o) &= F(2^{C_o} - 1) - \varepsilon \\ &\cong \prod_{i=0}^{N_t} \left[1 - \frac{1}{\sqrt{\pi} \Gamma(N_r)} \sum_{n=1}^{N_p} H_n \Gamma(N_r, (2^{C_o} - 1) c_{in}) \right] - \varepsilon \end{aligned} \quad (16)$$

where ε is the given outage probability. We now show that $G(C_o)$ is a monotonic function with $G'(C_o) > 0$. Differentiating $G(C_o)$ with respect to C_o gives

$$G'(C_o) = \frac{\partial G(C_o)}{\partial C_o} = f(2^{C_o} - 1) 2^{C_o} \ln 2 > 0 \quad (17)$$

Considering that 2^{C_o} , $\ln 2$ and the PDF $f(2^{C_o} - 1)$ are all positive, the derivative $G'(C_o)$ in (17) is also positive. Thus $F(C_o)$ is a strictly monotonically increasing function of C_o .

Substituting (11) into (17) yields

$$G'(C_o) \cong \sum_{i=0}^{N_t} \frac{1}{\Gamma(N_r)\sqrt{\pi}} \sum_{n=1}^{N_p} H_n \frac{(2^{C_o}-1)^{N_r-1} c_{in}^{N_r}}{e^{(2^{C_o}-1)c_{in}}} \prod_{k=0, k \neq i}^{N_t} \left[1 - \frac{1}{\sqrt{\pi}\Gamma(N_r)} \sum_{m=1}^{N_p} H_m \Gamma(N_r, (2^{C_o}-1)c_{im}) \right] \tag{18}$$

Eq.(18) is the closed-form expression of the derivative $G'(C_o)$. From (16), we can obtain

$$G(\infty) = \lim_{C_o \rightarrow \infty} G(C_o) = 1 - \varepsilon > 0 \tag{19}$$

and

$$G(0) = 0 - \varepsilon = -\varepsilon < 0 \tag{20}$$

This is because outage probability $\varepsilon \in (0, 1)$. Based on the analysis above, the equation $G(C_o)=0$ is shown to have a unique solution for $C_o>0$.

There are many methods such as bisection for finding the root of a strictly monotonic function. We propose to use Newton’s method to find the root iteratively because it has the quadratic convergence rate. Newton’s method is described as follows.

$$C_{o,l+1} = C_{o,l} - G(C_{o,l}) / G'(C_{o,l}) \tag{21}$$

where $C_{o,l}$ is the outage capacity value at the l -th iteration. $G(C_{o,l})$ and $G'(C_{o,l})$ are computed by (16) and (18), respectively. With (21), the accurate outage capacity can be achieved, and is shown to match the simulation well. However, this capacity needs iterative calculation. For this, we will give closed-form capacity calculation in the following.

With (11), we can calculate the second moment of the channel capacity $C=\log_2(1+\rho)$ as follows:

$$E(C^2) = \int_0^{+\infty} (\log_2(1 + \rho))^2 f(\rho) d\rho \cong \sum_{i=0}^{N_t} \sum_{n=1}^{N_p} H_n \sum_{u=1}^{N_q} A_u [\log_2(1 + z_u / c_{in})]^2 \frac{z_u^{N_r-1}}{\Gamma(N_r)\sqrt{\pi}} \prod_{k=0, k \neq i}^{N_t} F_{\rho_k} \left(\frac{z_u}{c_{in}} \right) \tag{22}$$

From (13) and (22), the variance of C can be evaluated as

$$V_c = E(C^2) - [E(C)]^2 = E(C^2) - C_e^2 \tag{23}$$

With the mean value (13) and the variance (23), using a Gaussian distribution approximation, the CDF of C can be approximated as

$$F(c) \approx \int_{-\infty}^c \frac{1}{\sqrt{2\pi V_c}} \exp\left(-\frac{(y - C_e)^2}{2V_c}\right) dy = 1 - 0.5 \operatorname{erfc}\left\{ \frac{c - C_e}{\sqrt{2V_c}} \right\} \tag{24}$$

where $\operatorname{erfc}\{ \cdot \}$ denotes the complementary error function. By setting the above $F(c)$ equal to the given outage probability ε , the outage capacity can be obtained as

$$C_o \approx \sqrt{2V_c} \operatorname{erfc}^{-1}\{2(1 - \varepsilon)\} + C_e \tag{25}$$

where $\operatorname{erfc}^{-1}\{ \cdot \}$ denotes the inverse complementary error function which can be evaluated by table look-up. Equation (25) is a closed-form expression of outage capacity, and has the value

close to the simulation. From (25) and (15), it is found that C_o will increase as ε increases, and decreases as ε decreases, which accords with the existing knowledge. Thus, the derived theoretical formulae provide an effective method to evaluate the outage performance of DAS downlink. Moreover, (25) is relatively simpler since it may provide closed-form calculation and does not need any iterative calculation.

4. BER performance analysis

Considering that BER is an another important performance measure of communication systems in fading channel, we will give the BER performance analysis of the DAS over composite fading channel in this section, and derive the average BER expressions of the system with MQAM and MPSK, respectively. For the given SNR ρ , utilizing [37, Eq.(16)] and [38, Eq.(8)], the average BER of DAS with MQAM and Gray codes can be given by

$$\begin{aligned} P_{b,q} &= \int_0^\infty f(\rho) \sum_l \xi_l \operatorname{erfc}\{\sqrt{\tau_l \rho}\} d\rho = \sum_l \xi_l \int_0^\infty \operatorname{erfc}\{\sqrt{\tau_l \rho}\} dF(\rho) \\ &= \sum_l \xi_l \int_0^\infty F(\rho) e^{-\tau_l \rho} \sqrt{\tau_l / (\pi \rho)} d\rho = \sum_l \xi_l \int_0^\infty F(z / \tau_l) e^{-z} / \sqrt{\pi z} dz \end{aligned} \quad (26)$$

where ξ_l and τ_l are constants which depend on M (i.e., the constellation size), and the constant sets $\{\xi_l, \tau_l\}$ for MQAM can be found in [37][32]. $f(\rho)$ and $F(\rho)$ are the PDF and CDF of ρ , respectively.

Using (10) and the Gauss-Laguerre integration [33], (26) can be changed to

$$\begin{aligned} P_{b,q} &\cong \sum_l \sum_{u=1}^{N_q} (\xi_l A_u / \sqrt{\pi z_u}) F(z_u / \tau_l) \\ &= \sum_l \sum_{u=1}^{N_q} \frac{\xi_l A_u}{\sqrt{\pi z_u}} \prod_{i=0}^{N_l} \left[1 - \frac{1}{\sqrt{\pi} \Gamma(N_r)} \sum_{n=1}^{N_p} H_n \Gamma(N_r, z_u c_{in} / \tau_l) \right] \end{aligned} \quad (27)$$

where $c_{in} = 10^{-[\sqrt{2}\sigma_{in} + \nu_i]/10}$. Eq.(27) is a tightly-approximate closed-form expression of average BER of DAS with MQAM over composite fading channel.

In the following, we give the derivation of average BER of DAS with MPSK. According to [39, Eq.(12)] and [38, Eq.(1)], the average BER using MPSK and Gray codes can be expressed as

$$\begin{aligned} P_{b,p} &\cong \frac{1}{\max(\log_2 M, 2)} \sum_{l=1}^{\max(M/4, 1)} \int_0^\infty f(\rho) \operatorname{erfc}(\sqrt{\zeta_l \rho}) d\rho \\ &= \frac{1}{\max(\log_2 M, 2)} \sum_{l=1}^{\max(M/4, 1)} \int_0^\infty F(\rho) \sqrt{\zeta_l / (\pi \rho)} e^{-\tau_l \rho} d\rho \end{aligned} \quad (28)$$

where $\zeta_l = \sin^2((2l-1)\pi/M)$, and M is the constellation size. Using (10) and the Gauss-Laguerre integration [33], (28) can be rewritten as

$$P_{b,p} \cong \frac{1}{\max(\log_2 M, 2)} \sum_{l=1}^{\max(M/4, 1)} \sum_{u=1}^{N_q} \frac{A_u}{\sqrt{\pi z_u}} \prod_{i=0}^{N_l} \left[1 - \frac{1}{\sqrt{\pi} \Gamma(N_r)} \sum_{n=1}^{N_p} H_n \Gamma(N_r, z_u c_{in} / \zeta_l) \right] \quad (29)$$

Eq.(29) is a tightly-approximate closed-form expression of average BER of DAS with MPSK over composite fading channel. Eqs.(27) and (29) provide closed-form calculations of the system BER in theory, and have more accuracy than the existing expression in [30]. It is because the latter employs the gamma distribution to approach the log-normal shadowing in (5) for the derivation of PDF and BER, which will result in the inaccuracy of the derived BER in some cases. Besides, unlike the derived BER in [31], the expression is limited in BPSK modulation. It is shown that (27) and (29) will be very close to the corresponding simulated values. Hence, using them, the error performance of DAS with MQAM and MPSK will be effectively evaluated.

5. Simulation Results and theoretical evaluation

In this section, we use the derived theoretical performance formulae and computer simulation to evaluate the capacity and BER performance of the DAS over composite channels, where path loss, Rayleigh fading and lognormal shadowing are all considered. In simulation, for analytical convenience, the cell shape is assumed to be circle with radius R . The BS (RA_0) is in the center of the cell, and the N_r RAs are uniformly distributed over a circle with radius d . Correspondingly, the polar coordinate of the i th RA is $(d, 2\pi(i-1)/N_r)$, $i=1,2,\dots,N_r$. The main parameters are listed as: $N_r=6$; $d=2R/3$; the reference distance $d_r=50m$; radius of the cell $R=10^3m$. The simulation results are illustrated in Figs.2-8.

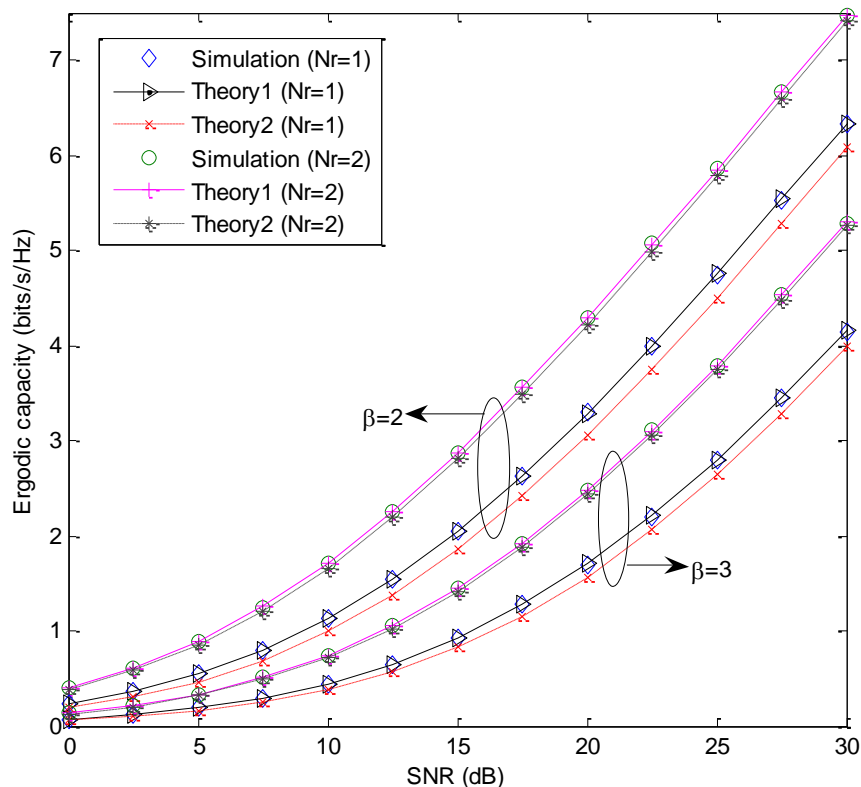


Fig. 2. Ergodic capacity of DAS with different receive antennas and path loss exponents ($N_r=1,2$, $\beta=2,3$, $\sigma=8dB$)

In Fig. 2, we plot the theoretical ergodic capacity and corresponding simulation of the DAS system with different receive antennas and path loss exponents, where standard deviation $\sigma=\sigma_i=8\text{dB}$. The derived (13) is used for theoretical calculation (referred as ‘theory 1’), and the existing theoretical formula [18][19] (referred as ‘theory 2’) is used for comparison. As shown in Fig.2, the theoretical values from ‘theory 1’ are all in good agreement with the simulated ones for different receive antennas and path loss cases. Whereas the theoretical values from ‘theory 2’ have some difference with the corresponding simulations, and the difference will be more obvious when the antenna number is smaller. This is because the latter uses the log-normal distribution to replace the Gamma-log-normal distribution for deriving the PDF, which brings about the inaccuracy of the derived ergodic capacity in some cases. Thus, our derived ‘theory 1’ has more accuracy. Besides, it is observed that the systems with $N_r=2$ outperform those with $N_r=1$ because the former has greater diversity than the latter, and the ergodic capacity of DAS with $\beta=3$ is lower than that with $\beta=2$ due to larger path loss, as expected. The above results show that the derived capacity expression of DAS is effective and reasonable.

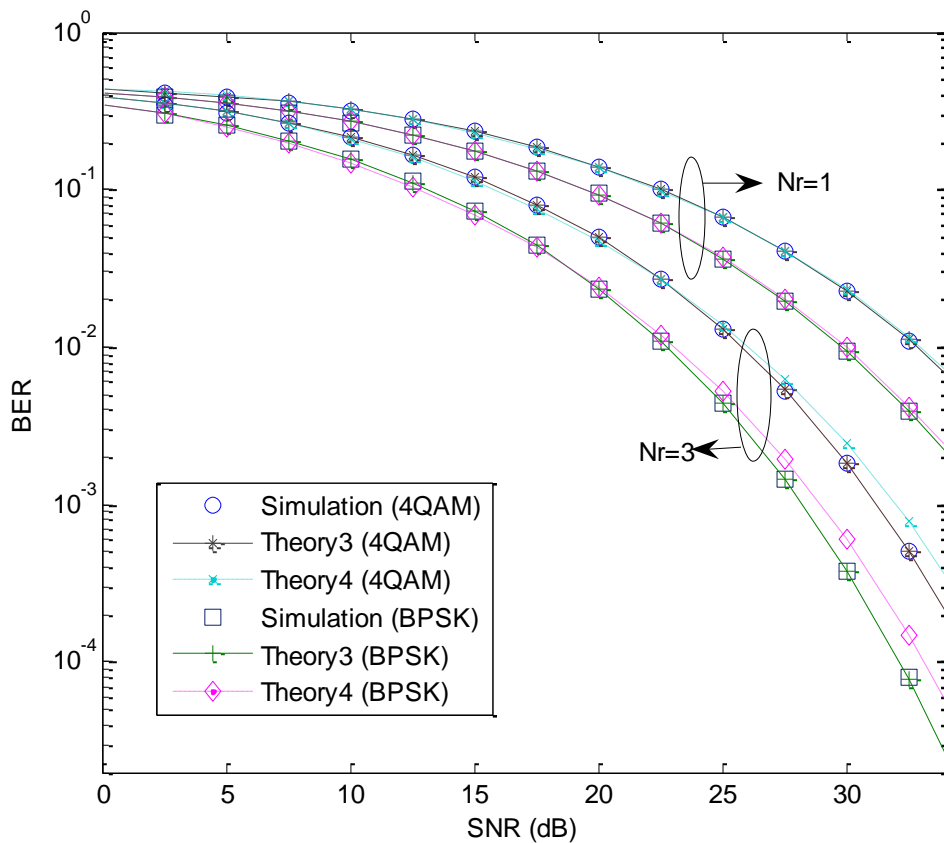


Fig. 3. Average BER of DAS with different receive antennas and modulation modes ($\beta=3$, $\sigma=8\text{dB}$, $N_r=1,3$).

In Fig. 3, we plot the theoretical average BER and corresponding simulation of DAS with different receive antennas and modulation modes, where standard deviation $\sigma=8\text{dB}$, path loss exponent $\beta=\beta_i=3$, BPSK and 4QAM are used for the system modulation. The theoretical BER

are evaluated by (27) and (29) for 4QAM and BPSK modulation respectively, which is referred as ‘theory 3’. For comparison, the existing theoretical formula [30] (referred as ‘theory 4’) is also employed for BER calculation. It is found that the derived ‘theory 3’ can match the corresponding simulation very well, whereas the existing ‘theory 4’ is close to the simulated value for single receive antenna case only. When the number of the receive antenna is large, the ‘theory 4’ will be different with the simulation. The reason for this is that ‘theory 4’ uses the gamma distribution instead of the log-normal shadowing to derive the PDF and the corresponding BER. As a result, the obtained BER is not accurate. Besides, the average BER of DAS with three receive antennas is lower than that with single receive antenna due to the achievable higher diversity gain. Moreover, the BER performance of DAS with BPSK is superior to that of DAS with 4QAM. It is because the latter employs higher modulation, while the constellation points in high modulation are densely packed and prone to errors in fading channel. The above results indicate that the derived BER expression of DAS is also valid for error performance evaluation.

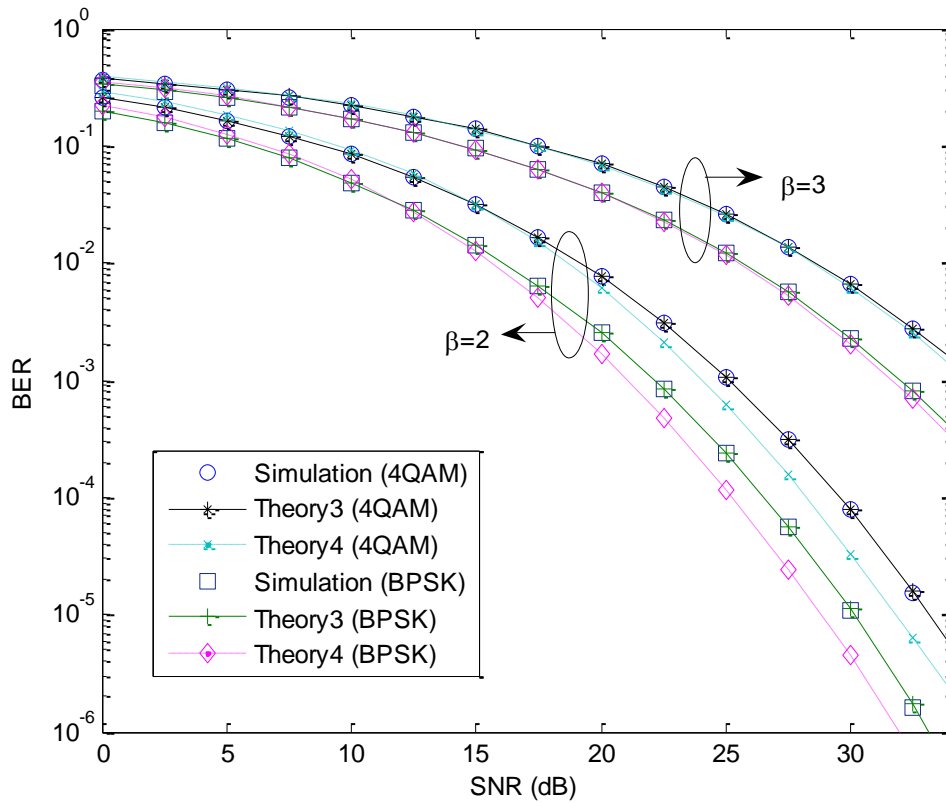


Fig. 4. Average BER of DAS with two receive antennas and different path-loss exponents ($N_r=2$, $\sigma=10\text{dB}$, $\beta=2,3$)

Fig. 4 shows the BER performance of DAS with two receive antennas and different path loss exponents, where $\sigma=10\text{dB}$, 4QAM and BPSK are used. The ‘theory 3’ and ‘theory 4’ are employed for theoretical calculation of average BER. As shown in Fig.4, the derived ‘theory 3’ still has the values very close to the corresponding simulated ones, but the theoretical evaluation from ‘theory 4’ is different with the simulation result. Especially for small path loss exponent case, the difference is much more obvious. Besides, it is found that DAS with $\beta=3$ is

worse than that with $\beta=2$ because larger path loss happens, which accords with the existing knowledge. The above results further testify that the derived BER formulae are effective and reasonable.

In Fig. 5, we plot the theoretical BER and corresponding simulation of DAS with different high modulations and four receive antennas, where $\sigma=10\text{dB}$, $\beta=2$, 8PSK and 16QAM are employed for modulation. The ‘theory 3’ and ‘theory 4’ are used for theoretical evaluation. From Fig.5, we can see that our ‘theory 3’ can still match the simulation well, but the ‘theory 4’ has obvious difference with the simulation. Besides, the BER performance of DAS with 16QAM is worse than that of DAS with 8PSK. This is because the former employs higher modulation, and will be easy to occur error under fading case. The above results show that the derived theoretical BER is also valid for higher order modulation.

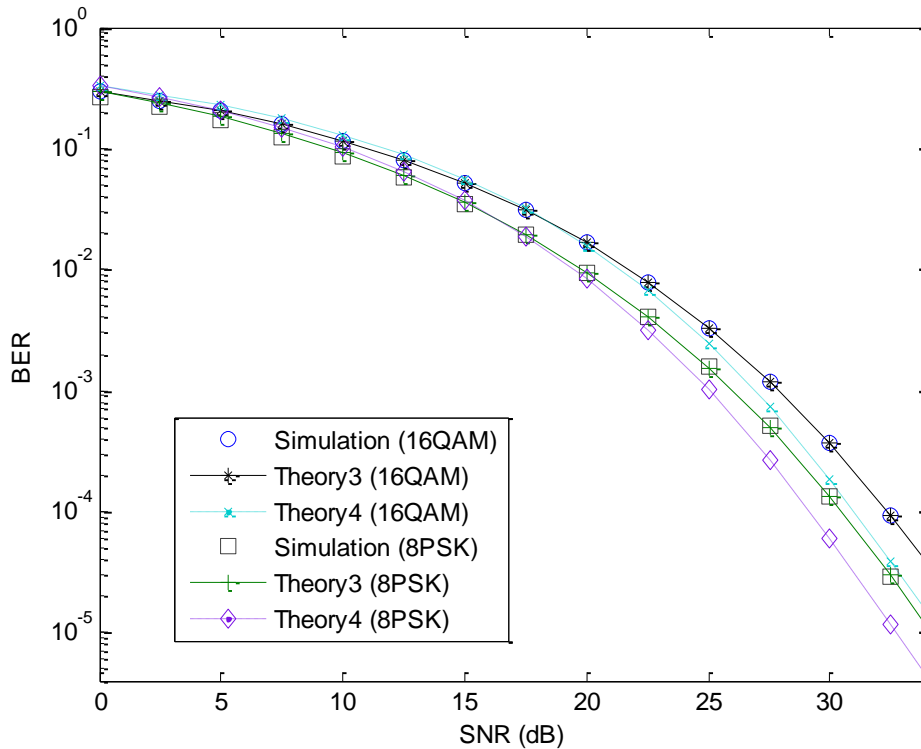


Fig. 5. Average BER of DAS with four receive antennas and modulations ($N_r=4$, $\beta=2$, $\sigma=10\text{dB}$).

In Fig. 6, we plot the theoretical outage capacity and corresponding simulation of DAS with different receive antennas and outage probability, where the outage probability P_o is set as 0.15 and 0.3, respectively. $\beta=3$, $\sigma=6\text{dB}$, and $N_r=2, 4$. The accurate and approximate outage capacities are respectively calculated by (21) and (25), and they are referred as ‘theory 5’ and ‘theory 6’, respectively. Computer simulation results verify the effectiveness of the derived theoretical formula, that is, the theoretical values are all close to the corresponding simulated ones. Especially, the ‘theory 5’ from the Newton’s method has more accuracy than the ‘Theory 6’ from Gaussian distribution approximation, but the latter does not need iterative calculation. It is observed that the outage capacity of DAS with four receive antennas is higher than that with two receive antennas under the same P_o because multiple antennas are employed.

Besides, under the same receive antenna number, the outage capacity of DAS with $P_o=0.3$ is higher than that with $P_o=0.15$ since larger outage probability is permitted to happen, which accords with the theoretical analysis in section 3.

Fig. 7 shows the outage capacity performance of DAS with three receive antennas under different path loss and outage probability, where $\sigma=6\text{dB}$, $\beta=2, 4$, and $P_o=0.15, 0.3$. ‘Theory 5’ and ‘theory 6’ are employed for the theoretical calculation of outage capacity. From this figure, we can find the results similar to Fig.6. Namely, the derived theoretical outage capacity can match the corresponding simulation well, only some little differences are observed for ‘theory 6’, and the outage capacity of DAS with large P_o is higher than that with small P_o . Besides, the outage capacity of DAS with $\beta=4$ is lower than that with $\beta=2$ since the former experiences larger path loss, which agrees with the existing knowledge as well. The above results show that the derived theoretical formulae are valid and reasonable.

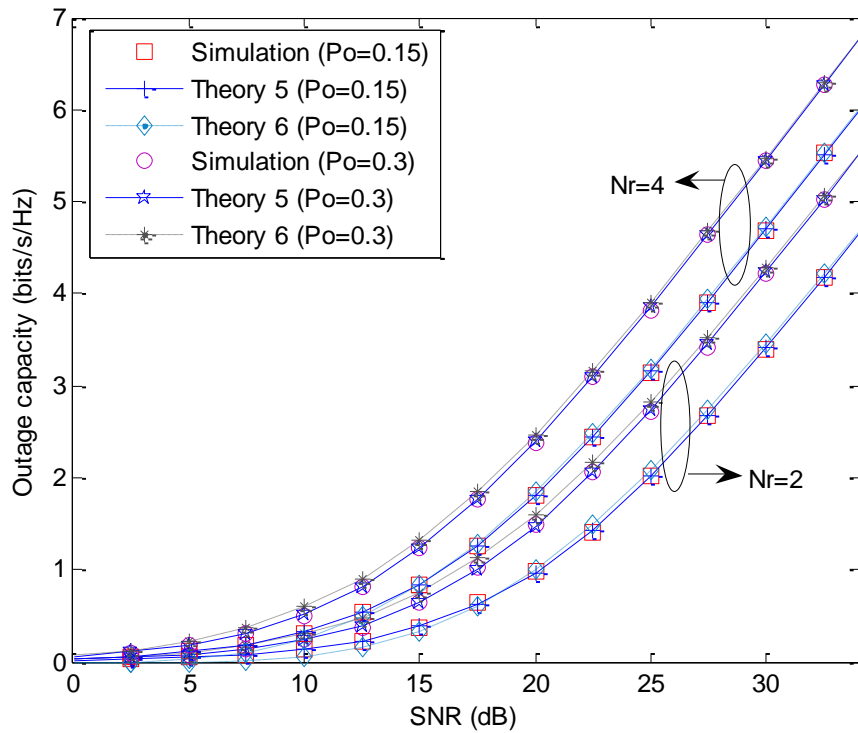


Fig. 6. Outage capacity of DAS with different receive antennas and outage probability ($\beta=3$, $\sigma=6\text{dB}$, $N_r=2, 4$, $P_o=0.15, 0.3$).

In **Fig. 8**, we plot the theoretical outage probability and corresponding simulation of DAS with different receive antennas and path loss exponents, where the outage capacity C_o is set as to 2bit/s/Hz , $\sigma=6\text{dB}$, and $\beta=2,3$. The theoretical outage probability is calculated by (15). As shown in Fig.8, the theoretical outage probability and the corresponding simulation result are very close to each other. It is found that the outage probability of DAS with three receive antennas is lower than that with two receive antennas since the former has greater diversity than the latter. Besides, due to larger path loss, the outage probability of DAS with $\beta=3$ is larger than that with $\beta=2$ as expected. The above results indicate that the derived outage probability is also valid for the outage performance evaluation.

6. Conclusion

We have studied the downlink performance of DAS over MIMO composite fading channel, and the capacity and BER as well as outage performance are all analyzed. Based on the performance analysis, using some numerical integrations, the PDF and CDF of the effective output SNR are respectively derived. With these results, the tightly-approximate closed-form expressions of ergodic capacity and average BER of DAS are achieved, respectively. These expressions have more accuracy than the existing ones, and obtain the values very close to the actual simulations. According to the outage performance analysis, a tightly-approximate closed-form expression of outage probability is also derived for a given outage capacity. Meanwhile, Newton's method is proposed to find the system outage capacity for a given outage probability. Moreover, to simplify the calculation of the outage capacity, an approximate closed-form expression of outage capacity of DAS is derived by using the Gaussian distribution approximation, which does not need any iterative calculation. Simulation result show that the presented theoretical analysis can match the corresponding simulations very well, and the system performance can be effectively improved as the number of receive antennas increases and/or path loss exponent decreases. Thus, these theoretical expressions provide good performance evaluation for downlink DAS in composite channel, and avoid the conventional requirement for Monte Carlo simulation.

Besides, we also notice that this paper only addresses the performance study of DAS in single-cell, whereas in practice, the DAS will operate in multi-cell scenario. Under multi-cell case, the inter-cell interference (ICI) will affect the system performance inevitably, and bring about the performance degradation. Considering the practicability, in the future work, we will further study the performance of the DAS in multi-cell scenario where ICI is considered. It is expected that some practical results can be achieved.

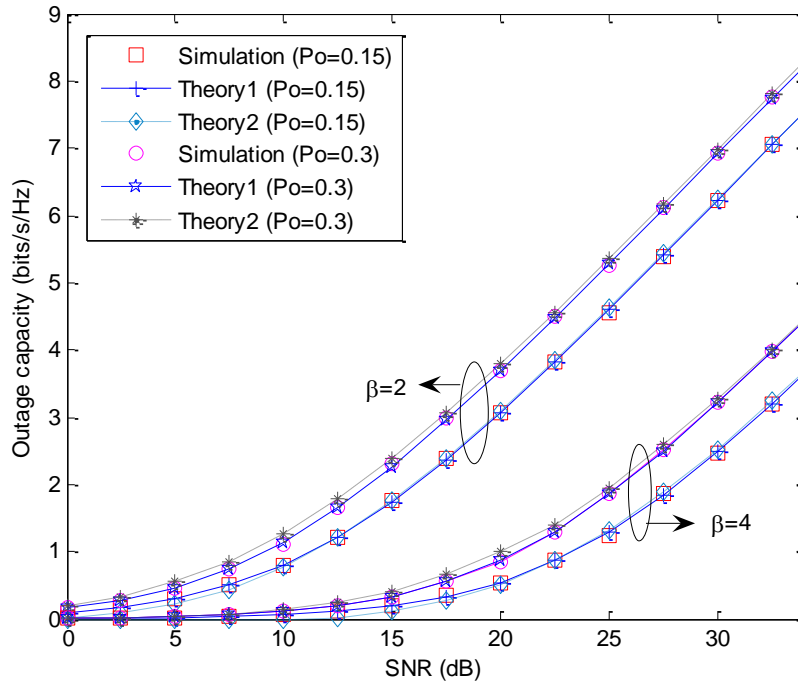


Fig. 7. Outage capacity of DAS with different path loss exponents and outage probability ($N_r=3$, $\sigma=6$ dB, $\beta=2, 4$, $P_o=0.15, 0.3$).

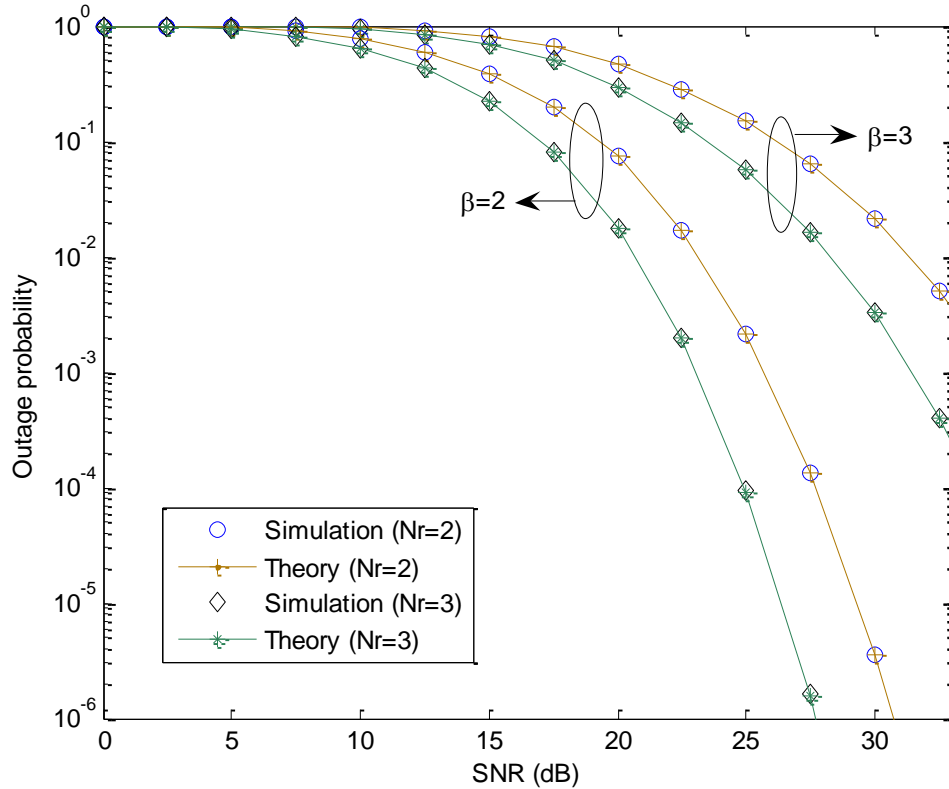


Fig. 8. Outage probability of DAS with different receive antennas and path loss exponents ($N_r=2, 3$, $\sigma=6\text{dB}$, $C_0=2\text{bit/s/Hz}$, $\beta=2, 3$).

Acknowledgment

The authors would like to thank three anonymous reviewers for their valuable comments and excellent suggestions which considerably improved the paper.

References

- [1] D. Castanheira, A. Gameiro, "Distributed antenna system capacity scaling," *IEEE Wireless Communication*, vol.17, pp.68-75, 2010. [Article \(CrossRef Link\)](#)
- [2] C.-X. Wang, X. Hong, X. Ge, X. Cheng, G. Zhang, J.S. Thompson, "Cooperative MIMO channel models: A survey," *IEEE Communications Magazine*, vol.48, no.2, pp. 80-87, 2010. [Article \(CrossRef Link\)](#)
- [3] J.-B. Wang, J.-Y. Wang, M. Chen, "Downlink system capacity analysis in distributed antenna systems," *Wireless Personal Communications*, vol. 67, pp. 631-645, 2012. [Article \(CrossRef Link\)](#)
- [4] X. Ge, K. Huang, C.-X. Wang, X. Hong, X. Yang, "Capacity analysis of a multi-cell multi-antenna cooperative cellular network with co-channel interference," *IEEE Transactions on Wireless Communications*, vol. 10, no. 10, pp.3298-3309, 2011. [Article \(CrossRef Link\)](#)
- [5] X. Hong, C.-X. Wang, M. Uysal, X. Ge, O. Shan, "Capacity of hybrid cognitive radio networks with distributed VAAs," *IEEE Transactions on Vehicular Technology*, vol.59, no.7, pp. 4201-4213, 2010. [Article \(CrossRef Link\)](#)
- [6] R. Heath, S. Peters, Y. Wang, J. Zhang, "A current perspective on distributed antenna systems for

- the downlink of cellular systems,” *IEEE Communications Magazine*, vol.51, no.4, pp. 161-167, 2013. [Article \(CrossRef Link\)](#)
- [7] H.Q.Gao, R.F.Song, “Distributed compressive sensing based channel feedback scheme for massive antenna arrays with spatial correlation,” *KSII Transactions on Internet and Information Systems*, vol.8, no.1, pp.108-122, 2014. [Article \(CrossRef Link\)](#)
- [8] X.-H.You, D.-M.Wang, B. Sheng, X.-Q. Gao, X.-S. Zhao, M. Chen, “Cooperative distributed antenna systems for mobile communications,” *IEEE Wireless Communications*, vol.17, no.3, pp. 35-43, 2010. [Article \(CrossRef Link\)](#)
- [9] 3GPP-LTE, “Technical specification group radio access network: Evolved universal terrestrial radio access (E-UTRA): further advancements for E-UTRA physical layer aspects (release 9),” 3GPP TR36.814, Mar. 2010.
- [10] F. Adachi, K. Takeda, T. Yamamoto, and R. Matsukawa, “Gigabit distributed antenna network and its related wireless techniques,” in *Proc. of International Wireless Communications and Mobile Computing Conference (IWCMC)*, 2011, pp. 1550–1556. [Article \(CrossRef Link\)](#)
- [11] S. Sanayei, A. Nosratinia, “Antenna selection in MIMO systems,” *IEEE Communication Magazine*, vol.42, pp. 68-73, 2004. [Article \(CrossRef Link\)](#)
- [12] Z.Chen, J.Yuan, B.Vucetic, “Analysis of transmit antenna selection/maximal-ratio combining in Rayleigh fading channel,” *IEEE Transactions on Vehicular Technology*, vol.54, no.4, pp. 1312–1321, 2005. [Article \(CrossRef Link\)](#)
- [13] L. Dai, S. Zhou, Y. Yao, “Capacity analysis in CDMA distributed antenna systems,” *IEEE Transactions on Wireless Communications*, vol.4, pp.2613-2620, 2005. [Article \(CrossRef Link\)](#)
- [14] W. Choi, J. D. Andrews, “Downlink performance and capacity of distributed antenna systems in a multicell environment,” *IEEE Transactions on Wireless Communications*, vol.6, pp. 69-73, 2007. [Article \(CrossRef Link\)](#)
- [15] Y. Liu, J. Liu, H. Chen, et al., “Downlink performance analysis of distributed antenna systems,” in *Proc. of IEEE Wireless Communications and Signal Processing*, pp.1-5, 2011. [Article \(CrossRef Link\)](#)
- [16] X.B. Yu, Y. Yang, M.Q. Li, M. Chen, “Capacity analysis of distributed antenna systems in MIMO Nakagami fading multicell environment,” *Annals of Telecommunications*, vol.67, pp.589-595, 2012. [Article \(CrossRef Link\)](#)
- [17] J. Park, E. Song, W. Sung, “Capacity analysis for distributed antenna systems using cooperative transmission schemes in fading channels,” *IEEE Transactions on Wireless Communications*, vol.8, pp. 586-592, 2009. [Article \(CrossRef Link\)](#)
- [18] J. Wang, J. Wang, X. Dang, et al., “System capacity analysis of downlink distributed antenna systems over composite channels,” in *Proc. of IEEE International Conference on Communication Technology*, pp.1076-1079, 2010. [Article \(CrossRef Link\)](#)
- [19] H. Chen and M. Chen, “Capacity of the distributed antenna systems over shadowed fading channels,” in *Proc. of Proceedings of the IEEE Vehicular Technology Conference*, pp. 1-4, 2009. [Article \(CrossRef Link\)](#)
- [20] Y.Wen, J.Wang, M. Chen, “Ergodic capacity of distributed antenna systems over shadowed Nakagami-m fading channels,” in *Proc. of IEEE Wireless Communications and Signal Processing*, pp.1-6, 2013. [Article \(CrossRef Link\)](#)
- [21] S.-R. Lee, S.-H. Moon, J.-S. Kim, I. Lee, “Capacity analysis of distributed antenna systems in a composite fading channel,” *IEEE Transactions on Wireless Communications*, vol. 11, no. 3, pp.1076-1086, 2012. [Article \(CrossRef Link\)](#)
- [22] M. Matthaiou, N.D. Chatzidiamantis, G.K.Karagiannidis, “A new lower bound on the ergodic capacity of distributed MIMO systems,” *IEEE Signal Processing Letters*, vol.8, pp.227-230, 2011. [Article \(CrossRef Link\)](#)
- [23] W. Roh and A. Paulraj, “Outage performance of the distributed antenna systems in a composite fading channel,” in *Proc. of IEEE Vehicular Technology Conference*, vol.3, pp. 1520-1524, 2002. [Article \(CrossRef Link\)](#)
- [24] J.Wang, J.Wang, M. Chen, et al., “System outage probability analysis of uplink distributed antenna systems over a composite channel,” in *Proc. of IEEE 73rd Vehicular Technology Conference*, pp.

- 1-5, 2011. [Article \(CrossRef Link\)](#)
- [25] H. Chen, J. Wang, M. Chen, "Outage performance of distributed antenna systems over shadowed Nakagami-m fading channels," *European Transactions on Telecommunications*, vol.20, pp. 20:531-535, 2009. [Article \(CrossRef Link\)](#)
- [26] J. Cai, X. Zhao, J.Wang , M.Gu, "Probabilistic analysis of system outage in distributed antenna systems with composite channels," *EURASIP Journal on Wireless Communications and Networking*, vol.2013, no.1, article 147, 2013. [Article \(CrossRef Link\)](#)
- [27] J.Wang, M.Chen, Q.-S. Hu. "System outage probability analysis of distributed antenna systems over shadowed generalized-gamma composite channels," in *Proc. of IEEE Wireless Communications and Signal Processing*, pp.1-6, 2012. [Article \(CrossRef Link\)](#)
- [28] H. Chen, J.Wang, M. Chen, "Outage capacity study of the distributed MIMO system with antenna cooperation," *Wireless Personal Communications*, vol. 59, no.4, pp.599–605, 2011. [Article \(CrossRef Link\)](#)
- [29] F. Héliot, R. Hoshyar, R. Tafazolli, "A closed-form approximation of the outage probability for distributed MIMO systems," in *Proc. of IEEE 10th Workshop on Signal Processing Advances in Wireless Communications*, pp.529-533, 2009. [Article \(CrossRef Link\)](#)
- [30] H. Chen, J. Wang, M.Chen, "Performance analysis of the distributed antenna system with antenna selective transmission over generalized fading channels," in *Proc. of IEEE Wireless Communications and Signal Processing*, pp.1-4, 2009. [Article \(CrossRef Link\)](#)
- [31] Y.Liu, J. Liu, W. Guo, et al., "Outage probability and bit-error rate analysis of distributed antenna systems in multicell environment," *IET Communications*, vol.7, pp. 791 -798. 2013. [Article \(CrossRef Link\)](#)
- [32] M. K. Simon, M. S. Alouini, *Digital Communication over Fading Channels*, New York: Wiley, 2005.
- [33] M.Abramowitz, I. A. Stegun, *Handbook of mathematical functions: with formulas, graphs, and mathematical tables*. Courier Dover Publications, 2012.
- [34] I. S. Gradshteyn and I. M. Ryzhik, *Table of integrals, series, and products*, 7th ed. San Diego, CA: Academic, 2007.
- [35] E. Biglieri, R.Calderbank, A. Constantinides, et. al., *MIMO wireless communications*. Cambridge, U.K.: Cambridge Univ. Press, 2007.
- [36] E.G.Larsson, P.Stoica, *Space-time block coding for wireless communications*. Cambridge, U.K.: Cambridge Univ. Press, 2003.
- [37] K. Cho, D. Yoon, "On the general BER expression of one-and two-dimensional amplitude modulations," *IEEE Transactions on Communications*, vol.50, no.7, pp. 1074-1080, July 2002. [Article \(CrossRef Link\)](#)
- [38] X. Yu, S-H. Leung, X.Chen, "Performance analysis of space-time block coded MIMO systems with imperfect channel information over Rician fading channels," *IEEE Transactions on Vehicular Technology*, vol.60, pp. 4450- 4461, 2011. [Article \(CrossRef Link\)](#)
- [39] J.Lu, K.B.Letaief, J.C.I.Chuang, et al., "M-PSK and M-QAM BER computation using signal-space concepts," *IEEE Transactions on Communications*, vol.47, pp.181-184, 1999. [Article \(CrossRef Link\)](#)



Weiye Xu received the B.S. degree in Communication Engineering from Hohai University, China, in 2001, and the M.S. degree in Communication and Information Systems from Hohai University, Nanjing, China, in 2007. She is currently a Lecturer in School of Communication Engineering at Nanjing Institute of Technology. Her research interests include digital communication, MIMO technique, distributed antenna systems.



Qingyun Wang received the M.S. degree from Southeast University, Nanjing, China in 2002 and the Ph.D. degree in Signal and Information Processing from Southeast University in 2011. She is currently an Associate Professor in School of Communication Engineering at Nanjing Institute of Technology. Her research interests include digital communication, speech signal processing.



Ying Wang received the B.S. degree in electrical engineering from Nanjing University of Aeronautics and Astronautics, Nanjing, China, in 2014, she is currently working towards the M.S. degree at Nanjing University of Aeronautics and Astronautics.



Binbin Wu received the B.S. degree in electrical engineering from Nanjing University of Aeronautics and Astronautics, Nanjing, China, in 2013, he is currently working towards the M.S. degree at Nanjing University of Aeronautics and Astronautics.